Subcellular Localization Analysis of Truncation Mutants of Porcine Circovirus 1 VP3

A Major Qualifying Project

Submitted to the faculty of

WORCESTER POLYTECHNIC INSTITUTE

in partial fulfillment of the requirements for the

Degree of Bachelor of Science

in Biochemistry

by

_____

Meaghan Paris

_____

Matija Zelic

April 28, 2011

Approved:

_____

Dr. Destin Heilman, Advisor

Department of Chemistry and Biochemistry, WPI

Abstract

Porcine Circovirus 1 (PCV1), a non-virulent member of the *Circoviridae* family, has been found to possess similar genome organization to Chicken Anemia Virus (CAV) and PCV2. The VP3 protein of these viruses selectively induces apoptosis strictly in transformed cells. Though the nuclear export signals (NES) and protein sequences exhibit homology, PCV1 VP3 has an elongated C-terminus tail domain compared to CAV VP3 and PCV2 VP3. In order to elucidate the relationship between the structure and function of PCV1 VP3, truncation mutants isolating the elongated tail domain and the NES were developed. Expression of GFP-tagged PCV1 VP3 in primary and transformed H1299 cell lines will show the functionality and localization patterns of these truncation mutants. Our research indicates that in transformed cells the tail domain has a distinctly cytoplasmic, vesicular localization while the NES is mainly found in the cytoplasm.

Acknowledgements

Table of Contents

Table of Figures

Background

Circoviridae

The *Circoviridae* family of viruses is identified by small, circular, single-stranded DNA structures. The family is composed of several species including the chicken anemia virus (CAV), porcine circoviruses (PCV1 and PCV2), goose circovirus (GoCV), and beak and feather disease virus (BFDV). CAV is the only member of the genus *Gyrovirus*. The others, sharing many structural and functional properties, are members of the genus *Circovirus*[22]. Though all these species are members of the same family, they produce various levels of pathology in different animals.

Porcine circovirus was originally discovered in 1974 as a nonpathogenic contaminant of the kidney cell culture in swine. Later characterized as PCV1, it is widespread in swine but not linked to any disease. A second strain was identified in 1991. PCV2 is associated with postweaning multisystemic wasting syndrome (PMWS), a disease affecting pigs between 5 and 18 weeks old. PMWS is an immunodeficiency-related disease with symptoms of weight loss, anemia, dyspnea, and jaundice. Interestingly, PCV2 has two highly homologous isoforms; PCV2a is nonpathogenic but the PCV2b isoform is linked to PMWS[10].

Similar to PCV2b, the chicken anemia virus also has pathogenic effects, causing increased mortality in young chickens. First discovered in the United States in 1979, the virus causes disease symptoms such as anemia, hemorrhage, and decreased resistance to bacterial disease, thus compromising the immune system. Severely affected birds die within 2 to 4 weeks of age while the growth of survivors is stunted[23]. The differing levels of pathologies between the members of the *Circoviradae* family are likely due to structural variations in the viruses. Thus, pathology may be due to potential differences in the viral capsids.

Structure

All the members of the *Circoviridae* family have been classified due to their circular genomes and small size. Therefore, it would be expected that the members of the family would be structurally similar. However, a closer look at the viral capsids shows a wide variation in their structure. The CAV capsid, as seen in Figure 1A, appears to have

trumpet-shaped capsomeres, protruding to an overall radius of 12.5nm. The image of the PCV2 capsid appears to be fairly dissimilar (Figure 1B). PCV2 particles are smaller, with pentamer units extending only 10.25nm, and have a much smoother surface than CAV. The CAV capsid has a mass of 50 kDa, while PCV2's capsid is only 28 kDa. Thus, the capsids of these proteins vary greatly in their structure and size, yet both species have pathogenic effects. Interestingly, the PCV1 and PCV2 capsid proteins share 66% sequence homology, but the strains differ in their pathogenicity[6]. However, PCV2a is nonpathogenic, while the PCV2b strain is associated with PMWS in swine[10]. It is obvious that the pathological differences observed among members of the *Circoviridae* are not due to structural differences in the capsid. Thus, the cause of pathogenic variance must lie within genomic structure differences between the circoviruses.

Genome Organization

Circoviruses are icosahedral, non-enveloped particles that have a diameter of 16-18 nm[26]. The viruses have small genomes around 2 kb, and are closed-circular, single-stranded DNA genomes[9]. CAV has a negative strand genome, while both PCV1 and PCV2 have ambisense genomes[6]. The genomes of the circoviruses, specifically PCV1 and PCV2, contain two major open reading frames (ORFs). ORF1 codes for replication process proteins (Rep and Rep') while the capsid protein is encoded by ORF2[9, 25]. The genomic organization of CAV differs slightly as its ORF1 encodes the large VP1 capsid protein. The C-terminal region of VP1 is associated with replication domains. Meanwhile, the ORF2 encodes a small, non-structural protein with a phosphatase domain[6]. However, the genomes of the three viruses are similar, with PCV1 and PCV2 expressing 76% homology[5].

Interestingly, the most conserved sequences lie within a third open reading frame, ORF3, which is present in all three viruses. ORF3 in CAV codes for a Virion Protein 3 (VP3) protein called apoptin[9]. In PCV, the third open reading frame is oriented in the opposite direction of ORF1 and is thought to encode for VP3. Approximately 81% of the PCV2 ORF3 nucleotide sequence is conserved in PCV1 ORF3[5]. Though the three viruses exhibit ORF3 sequence homology, the most notable difference is that the C-terminus of PCV1 has a unique "tail" domain that almost doubles the length of the protein compared to PCV2 VP3 or apoptin.

The ORF3 in CAV has been shown to cause apoptosis[8]. The apoptotic activity of this CAV open reading frame causes pathological effects seen in chickens. Similar to CAV ORF3, the PCV2b ORF3 encodes the VP3 protein which induces apoptosis, causing viral pathogenesis in swine[19]. Nonetheless, the similarity observed between the ORF3 sequences allows for comparison studies with PCV2b VP3 and CAV VP3, and raises the question as to whether PCV1 ORF3 codes for a similarly functioning VP3 protein.

VP3 and Apoptosis

The VP3 proteins in CAV and PCV2b have been shown to induce apoptosis and are associated with the pathological effects caused by these viruses[8, 19]. Interestingly, apoptin seems to be cancer cell specific. More precisely, it has been proven that apoptin induces apoptosis only in transformed cells[8]. Similarly, PCV2b VP3 shows cell-type specific apoptosis, as it induces apoptosis in transformed H1299 cells[2]. Furthermore, recent studies have shown that PCV1 VP3 also seems to be able to induce apoptosis in the H1299 cell line[5, 16]. Thus, CAV, PCV1, and PCV2b VP3-mediated apoptosis all seems to be p53-independent since the VP3 protein from all three viruses has been shown to cause apoptosis in H1299 cells, a p53 null non-small cell lung carcinoma cell line[2, 5, 11, 16]. To better comprehend the mechanisms of apoptotic induction of these viruses, the localization of VP3 needs to be understood.

Apoptin has been shown to localize to the cytoplasm in primary cells, but it exhibits a nuclear localization in transformed cells[7]. Meanwhile, recent studies in the Heilman lab have shown that PCV2b VP3 localizes to the cytoplasm in both primary foreskin fibroblasts (PFF) and transformed H1299 cells[2]. Additionally, the Heilman lab recently showed that PCV1 VP3 localizes to the cytoplasm in transformed H1299 cells[5]. All three VP3 proteins seem to induce apoptosis in transformed H1299 cells but their localization differs. While both apoptin and PCV2b VP3 are found in the cytoplasm of primary cells, apoptin localizes to the nucleus in transformed cells. However, both PCV1 VP3 and PCV2b VP3 still exhibit a cytoplasmic localization in transformed H1299 cells. This implies that the apoptotic mechanism of CAV VP3 differs from that of PCV2b VP3 and PCV1 VP3. Since both PCV2b VP3 and PCV1 VP3 exhibit similar localization and apoptotic activity in transformed cells, questions remain as to the importance of the

elongated tail region of PCV1 VP3 and the pathogenic difference of the two strains. The differences evident in the localization of these VP3 proteins indicate that nucleocytoplasmic shuttling may play a role in the apoptosis-induction mechanisms of the viruses.

Nucleocytoplasmic shuttling is important to the function of many proteins. Trafficking of proteins and macromolecules into and out of the nucleus occurs through nuclear pore complexes (NPCs), which span the inner and outer nuclear membrane. Stationary proteins called nucleoporins (nups) make up the NPCs and the FG repeats of certain nups are thought to create a permeability barrier. Karyopherin nuclear transport receptors bind signal sequences and interact with the FG repeats of nups to shuttle cargo into or out of the nucleus. Depending on their role, karyopherins are thus termed importins or exportins[13].

Importins recognize a nuclear localization signal (NLS) and bind the cargo in the cytoplasm to shuttle it into the nucleus. Most NLSs have a basic amino acid enriched region that can be either monopartite or bipartite. Exportins recognize a nuclear export signal (NES) and bind the cargo to shuttle it out of the nucleus. CRM1 is a common exportin that recognizes leucine-rich or hydrophobic-rich regions of the NES which are found in a large number of nucleocytoplasmic shuttling proteins[13]. The GTPase Ran is necessary for the mediation of loading and unloading of the cargo molecules. In nuclear export, RanGTP binds to the exportin-cargo complex and shuttles it into the cytoplasm. RanGAP hydrolyzes RanGTP, thus disassembling the complex and releasing the cargo. Exportin and RanGDP are transported back to the nucleus by NTF2, where RCC1 replenishes RanGTP. During nuclear import, RanGTP dissociates the importin-cargo complex once it enters the nucleus. Thus the RanGTP gradient is crucial for the nucleocytoplasmic shuttling of proteins bound to importins or exportins[13].

This shuttling pathway is used by apoptin, whose nuclear localization and nucleocytoplasmic shuttling activity in transformed cells is necessary for apoptosis induction[12]. The differing localization of apoptin in dissimilar cell types signifies the presence of nuclear localization signal (NLS) and nuclear export signal (NES) sequences. The putative NES and NLS sequences have been studied and identified in apoptin and PCV2 VP3. The NES in apoptin is located in the N-terminus, comprised of the amino

acid residues 37 to 46. The NLS is made up of two separate domains rich in lysine and arginine residues. This bipartite sequence includes the residues 86-88 and 116-118[12].

The NES in PCV2b VP3 is reported to contain the amino acid residues 38-48, a highly conserved region compared to apoptin. The NLS is not as close in similarity, but this does not exclude the presence of an NLS in PCV2b VP3[2]. Based on the homology of the ORF3s, putative NES and NLS sequences were most recently discovered in PCV1. The NES of PCV1 VP3 is presumed to be highly homologous to those of PCV2b VP3 and apoptin, comprised of the amino acid residues 38-49. The NLS is less clear, but lysine and arginine rich sequences like those found in apoptin show the putative NLS may encompass residues 65-68[5, 16]. The functions of these localization and export sequences are vital in the apoptosis inducing mechanism of apoptin. Due to shared sequence homology, PCV1 VP3 and PCV2b VP3 may include similar NES and NLS regions, with similar functions as those found in apoptin. To better characterize VP3-induced apoptosis, the basic mechanisms of apoptotic induction in cells need to be understood.

Apoptosis, or programmed cell death, is a natural process that occurs in multicellular organisms to regulate cells during normal development and homeostasis. Cells may be removed due to genetic damage or tissue remodeling and repair. Apoptosis can be induced in response to DNA damage or death signals received by the cell membrane and starts with bulge formation ("blebbing") and condensation of the nuclear and plasma membranes, detachment from surrounding cells, and condensation of the chromatin. Apoptotic progression leads to cytoskeletal disruption, endonucleolytic DNA cleavage, and cytoplasmic and cellular organelle shrinking and fragmenting into "apoptotic bodies". These membrane bound structures are quickly phagocytosed by nearby macrophages without inducing inflammation since cytokines aren't released by the phagocytes[14].

When cell damage due to double strand DNA breaks or other genotoxic events is detected, expression of the DNA-binding p53 transcription factor is up-regulated. This triggers a cascade which results in cellular growth arrest or initiation of the apoptotic pathway. Under normal cellular conditions, low concentrations of the p53 protein are found in the cytosol as its transcription is downregulated by MDM2. This transcription

5

factor binds to p53, decreasing the activity and speeding up the degradation of the protein. However, DNA damage results in the phosphorylation of the p53 protein, thus greatly increasing its activity and reducing its interaction with MDM2. By binding to DNA, the p53 protein assesses the genetic damage present in the cell and initiates G_1 cell cycle arrest to give the cell machinery time to repair its DNA. In the case of irreparable DNA damage p53 initiates the apoptotic pathway[14].

The blc-2/bax gene family is crucial in p53-regulated apoptosis induction. The pro- and anti-apoptotic proteins of this gene family can both homo- and hetero-dimerize and p53 is hypothesized to control their levels of expression. High Bax expression promotes apoptosis while high Bcl-2 expression has the opposite effect. Bcl-2 proteins are important in ion transport and membrane integrity of the mitochondria so they're located on the cytosolic side of the outer membrane. Bax proteins are found in the cytosol but their increased expression forces them to bind to the mitochondrial membrane where they cause loss of selective ion permeability. Bax binding releases the contents of the mitochondrial intermembrane space into the cytoplasm. Apoptosis inducing factor (AIF) moves to the nucleus to initiate the condensation of chromatin. The leached cytochrome c is now able to bind and activate the cytoplasmic Apaf-1 protein, causing caspase activation. The downstream cascade activation of caspases results in the morphological changes and biochemical markers of apoptosis as caspases initiate and carry out the apoptotic process[14]. However, the problem with targeting the p53 apoptosis-inducing pathway for cancer therapeutics is that roughly half of all human tumors express a mutated p53[7, 24]. Interestingly, p53-independent apoptotic pathways also exist so these are being researched to look for potential cancer therapeutics that do not involve p53.

It is therefore of great intrigue that CAV VP3, PCV1 VP3, and PCV2b VP3-mediated apoptosis all seems to be p53 independent[2, 4, 11, 16]. In transformed cells, apoptin associates with subunit 1 (APC1) of the anaphase-promoting complex/cyclosome (APC/C). This interaction leads to G_2/M cell-cycle arrest and the initiation of apoptin-mediated p53-independent apoptosis[11]. The APC/C is a large multiprotein complex that helps regulate timely and orderly progression through mitosis. It's an E3 ubiquitin ligase that targets cyclins and other mitotic regulators for degradation so that mitosis can progress normally. APC/C must be bound to Cdc20 or Cdh1 in order to bind its

6

substrates[1]. However, apoptin's nucleocytoplasmic shuttling activity and cell type-specific localization is necessary for efficient association with APC1. Thus, the binding of the C-terminal domain of apoptin to APC1 disrupts the APC/C complex and inhibits its function, thus inducing G_2/M arrest and apoptin-mediated apoptosis[11].

Recent studies have proposed a putative mechanism for PCV2-induced apoptosis where the PCV2b VP3 binds pPirh2, a porcine E3 ubiquitin ligase. Normally Pirh2 ubiquitinates and degrades p53. However, the PCV2b VP3 interacts with the p53 binding domain of pPirh2 in the cytosol of transformed cells. This specific interaction destabilizes the protein and lowers its expression while simultaneously leading to increased p53 expression, which triggers the p53-dependent apoptotic pathway[19]. Though this putative mechanism involving pPirh2 is p53 dependent, PCV2b has been shown to be able to induce apoptosis in H1299 cells, which are p53 null[2]. Thus, more research is needed to fully uncover the PCV2 apoptosis-inducing mechanism and address whether it acts in a p53-dependent or p53-independent manner. However, the activation of a caspase cascade seems necessary in both p-53 mediated and p53 independent apoptosis.

Caspases exist as inactive zymogens, or proenzymes, so they must be activated to start performing their functions. The activation of these cysteine proteases is extremely important in apoptotic processes[8, 20]. Caspase activation occurs in a cascade manner, either by autocatalysis or proteolytic cleavage by other caspases, so caspases are divided into initiator or effector caspases[8]. Initiator caspase-2, caspase-8, caspase-9, and caspase-10 are activated by self-cleavage and subsequently cleave effector caspase-3, caspase-6, and caspase-7[14, 17].

Caspase activation occurs through two main signaling routes: the extrinsic death receptor or the intrinsic mitochondrial pathway. The extrinsic death receptor pathway activates the initiator caspase-8, which then cleaves and activates the effector caspase-3 and caspase-7[17, 20]. Meanwhile, cytochrome c leaching into the cytosol triggers the intrinsic mitochondrial pathway. Cytochrome c binds to Apaf-1 and this complex activates the initiator caspase-9, which subsequently cleaves the effector caspase-3[20]. Activated effector caspases cleave peptides only after specific aspartic acid residues. These peptides include cytoskeletal and structural proteins, DNA repair enzymes, transcription factors, protein kinases, and cell cycle regulation proteins, thus causing

cytoskeletal protein cleavage, disruption of the nuclear membrane and cell-cell contact, and DNA fragmentation[8, 14]. Curiously, caspase-3 also seems to be involved in VP3-mediated apoptosis.

The active effector caspase-3 has been found in cells undergoing apoptin-mediated apoptosis. Though it seems that upstream caspase-1 and caspase-8 activation isn't necessary, apoptin requires the activation of caspase-3, and possibly other effector caspases, for rapid apoptosis induction[8]. Though the mechanism of PCV2b VP3-induced apoptosis is still being uncovered, research has shown that it requires initiator caspase-8 activation, but not caspase-9. Caspase-8 in turn activates the effector caspase-3[17]. This finding is interesting since it doesn't involve caspase-9 activation of caspase-3, as occurs during cytochrome c release from mitochondria in the p53-induced apoptotic pathway[14].

The effector caspase-3 seems to play a role in CAV VP3 and PCV2b VP3-mediated apoptosis, even though the localization of the viral VP3 proteins differs in primary and transformed cells[2, 7, 8, 17]. Interestingly, PCV1 VP3 also seems to be caspase-3 dependent as the Heilman lab performed an apoptosis assay with a caspase-3-7 kit[16]. Therefore, though the putative apoptosis-inducing mechanisms are presumed to be different, the effector caspase-3 seems to be involved in the postulated mechanisms of the VP3 proteins. The sequence homology evident in CAV VP3, PCV2b VP3, and PCV1 VP3 raises the idea that PCV1 VP3 may possess related NES and NLS sequences and function in a manner similar to apoptin or PCV2b VP3 to induce apoptosis. Furthermore, the similar localization exhibited by PCV2b VP3 and PCV1 VP3 raises questions as to the pathogenic difference of the two strains, and the importance of the elongated tail domain of PCV1 VP3.

PCV1 VP3

The apoptotic mechanism of PCV1 VP3 is not fully understood and the function of the elongated C-terminus tail region is not known. However, its relatively close sequence homology with PCV2b VP3, similar cytoplasmic localization in transformed cells, and VP3-mediated apoptosis-inducing ability makes it an interesting candidate to study[2, 5, 16]. Elucidation of the mechanistic and biochemical differences between PCV1 and PCV2b will hopefully shed more light on the cytopathogenic difference in the swine

8

population. Similarly, both PCV1 VP3 and PCV2 VP3 proteins seem to be promising candidates for further study as cancer therapeutics. Thus, our interest is to interpret the relationship between the structure and function of several regions of the PCV1 VP3 protein, mainly the putative NES sequence and the C-terminal tail region. By making truncation mutants via PCR and ligating them to pEGFP vectors, we wish to determine the subcellular localization of the putative NES sequence and the C-terminal tail region and assess the functionality of these truncated regions. The caspase-3/7-dependent apoptosis assay on primary and transformed H1299 cells will illuminate the apoptotic abilities and enhance knowledge of the apoptosis-inducing mechanism of the PCV1 VP3 protein.

Materials and Methods

PCV1 ORF3 truncation mutant construction:

Template DNA PCV1 ORF3 regions were isolated and amplified by PCR, with primers designed from the consensus sequence for PCV1 ORF3 based on Clustal alignments performed previously in the Heilman lab[16]. Primers for the full-length PCV1 ORF3 that were previously created in the Heilman lab were used, and new primers for truncation mutant amplification were designed and ordered from IDT (Coralville, IA)[5]. Four primers were used to amplify two separate regions of the PCV1 ORF3, corresponding to ORF3 regions that encode for the putative NES sequence and the C-terminal hydrophobic tail domain of the VP3 protein.

For amplification of the NES truncation mutant, the sequence for the forward primer was 5' GC**G AAT TC**T ACA CCA TGG CTC ACT TTC AAA AG 3'. The sequence of the reverse primer was 5' GC**G GAT CC**T TAA GAA ATT TCC GCG GGC TG 3'. The EcoRI restriction site (bolded and underlined) was built into the 5' site of the forward primer, while the BamHI (bolded and underlined) was built into the 5' site of the reverse primer, along with a stop codon. The 5' BamHI site binds the template DNA, flanking the 3' region of the amplicon. If the N-terminal Adenine nucleotide of the ATG codon is counted as 1, the forward and reverse primers amplified nucleotides 1-189

of PCV1 ORF3. Thus, the amplicon has the EcoRI and BamHI restriction sites flanking the 5' and 3' sites of the region of interest.

To amplify the C-terminal tail domain, the sequence of the forward primer was 5' GC**G AAT TC**A TAT GTG GCC TTC TTT ACT G 3'. The sequence of the reverse primer was 5' CC**G GAT CC**T CAG TGA AAA TGC CAA G 3'. As mentioned above, EcoRI and BamHI restriction sites were built into the 5' site of the forward and reverse primers, so that these restriction sites flank the region of interest. Since the PCV2 ORF3 is 315 nucleotides long, the primers amplified nucleotides 316-621 of PCV1 ORF3, representing the hydrophobic C-terminal tail domain.

In addition, primers to amplify the PCV1 ORF3 region which may contain a putative NLS were designed. The sequence of the forward primer was 5' GC**G AAT TC**A CAC ATA CGT TAC AGG GAA C 3' while the the reverse primer was 5' GC**G GAT CC**C TAC TTA TCG AGT GTG GAG CTC 3'. These primers, with EcoRI and BamHI restriction sites built into their respective 5' sites, would flank the nucleotides 190-312 of PCV1 ORF3.

For the PCR reaction mixture, Promega's GoTaq Green Master Mix was used. It contains Taq DNA polymerase, dNTPs, $MgCl_2$, and reaction buffers. The PCR reactions contained 4 μL of the GoTaq Master Mix, 1 μL each of the forward and reverse primers, 1 μL of diluted GFP PCV1 VP3 template DNA (1:100), and 13 μL ddH_2O, for a total of 20 μL. The PCR algorithm on the BioRad MyCycler machine consisted of an initial 4 minute denaturing step at 95 °C, followed by 30 amplification cycles, each at 95°C for 30 seconds, 55°C for 30 seconds, and 72°C for 30 seconds. The reactions were then held at 72°C for 5 minutes, and allowed to cool before being retrieved from the PCR machine. The NES and tail PCR products of expected size were visualized by electrophoresis on a 0.9% agarose gel, stained with ethidium bromide. The DNA was purified from excised gel slices using the GeneClean Kit (MP Biomedicals, LLC).

Subcloning: The purified PCV1 NES and PCV1 tail truncation mutants were ligated into T-vectors with the Promega pGEM-T vector kit at a 1 μL:5 μL vector:insert ratio. The T-vector contains a lacZ start codon, lac operator, and constitutively expressed amp gene to allow for blue-white screening and ampicillin resistance. DH5α competent *E. coli* were transformed with the ligation products and grown overnight in a 37°C

incubator on LB agar plates coated with 0.100 mg/mL ampicillin, 0.1 mM IPTG, and 40 µg/mL Xgal. Positive colonies were inoculated and grown overnight in 4 mL LB media with ampicillin. The plasmid constructs were purified from 1.5 mL of inoculated culture using alkaline lysis minipreparation (Small Scale Plasmid DNA Preparation from Maniatis). The T-vector DNA was digested with EcoRI and BamHI at 37°C for 1 hour and then electrophoretically separated on a 0.9% agarose gel, stained with ethidium bromide. 20 µL of colonies with restriction fragments of the expected sizes were grown overnight at 37°C on a shaker in 100 mL LB media with 0.100 mg/mL ampicillin. The Promega Wizard Plus Midipreps DNA Purification System was used to harvest the plasmid DNA. The Midiprep purified DNA constructs were restricted with EcoRI and BamHI for 2 hours at 37°C to verify proper insertion of the NES and tail truncation mutants. The constructs were confirmed by DNA sequencing through Macrogen USA Inc.

Cloning and Transformation in GFP vector: Since sequencing had confirmed that the PCV1 NES and PCV1 tail truncation mutants had successfully been cloned into T vector, the fragments were excised by EcoRI and BamHI restriction digestion. Similarly, the pEGFP-C1 vector was restricted to linearize it. The restriction digests were electrophoretically separated on a 0.9% agarose gel, stained with ethidium bromide, and the DNA fragments of correct size were purified with the GeneClean Kit (MP Biomedicals, LLC). The pEGFP-C1 vector contains a cytomegalovirus (CMV) promoter, a gene for kanamycin resistance, and expresses target proteins with an N-terminal GFP tag. The PCV1 tail fragment was ligated into the GFP plasmid at a 1 µL:3 µL vector:insert ratio using T4 DNA ligase while the PCV1 NES fragment was ligated at a 1 µL:2 µL vector:insert ratio. The ligation reactions were run at 4°C for 24 hours. DH5α competent *E. coli* were transformed with the ligation products, plated, screened, amplified, and purified as previously described for T-vector in the *Subcloning* section above. The Promega Wizard Plus Midipreps DNA Purification System was used to harvest the pEGFP plasmid DNA. The Midiprep purified DNA constructs were restricted with EcoRI and BamHI to verify proper insertion of the NES and tail truncation mutants into the pEGFP vector.

Tissue Culture and Transfection into PFF and H1299 cell lines:

H1299 non-small cell lung carcinoma cells were grown and maintained in DMEM with 10% FBS. For transfection of PFF and H1299 cell lines, circular coverslips were added to each well in 6-well tissue culture plates and then coated with 2mL of pre-diluted media seeded with the passaged cells. After 24-hour growth, the six-well plates containing H1299 cells were transfected with the pEGFP-PCV1 NES and pEGFP-PCV1 tail plasmids, while the PFF cells were transfected with the pEGFP-PCV1 ORF3 construct previously made in the Heilman lab[5]. The Qiagen Effectene Transfection Reagent kit was used to transfect the cells. Each sample was done in duplicate, along with a pEGFP-C1 vector control. PFF cells to be used for an apoptosis assay were transfected in a Lonza Nucleofector machine with either the p3xFLAG vector control or the p3XFLAG-myc-CMV-26-PCV1 ORF3 construct previously made in the Heilman lab[5]. Following transfection, 200 μL of PFF cells in media were added to wells in a 96-well plate.

After 24 hours, the cells were fixed with 4% paraformaldehyde in PBS. DAPI (4',6'-diamidino-2-phenylindole) was used for nuclear staining. The fixed cells were mounted on slides with mounting media (50% glycerol; 100 mM Tris (pH 7.5); 2% DABCO), and imaged by epifluorescence and confocal microscopy.

Apoptosis Assay:

The 96-well plate containing the PFF cells transfected with the 3xFLAG vector control or the 3xFLAG-PCV1 ORF3 construct was incubated at 37°C for 24 hours. The Promega Apo-ONE Homogeneous Capase-3/7 Assay kit was used to measure the activation of apoptosis by full-length PCV1 VP3. 100 μL of media was taken out of each well and 100 μL of Caspase Substrate/Apo-One Caspase-3/7 Buffer was added (1:100 ratio). After an 18-hour incubation at room temperature in the dark, a fluorescence spectrometer was used to measure to assess the cell death of the FLAG control and FLAG-PCV1 ORF3 construct in primary cells. The background controls were subtracted out to normalize the data.

Results

The CAV, PCV1 and PCV2b viruses of the Circoviridae family all encode a VP3 protein[5, 7, 19]. Though the three viruses exhibit ORF3 sequence homology, the most notable difference is that the C-terminus of PCV1 has an elongated tail domain. Nucleocytoplasmic shuttling and nuclear localization of apoptin in transformed cells has been shown necessary for its ability to induce apoptosis[12]. Though apoptin has a cytoplasmic localization in primary cells, it localizes to the nucleus in H1299 cells[7]. Previous studies in the Heilman lab indicated that a pEGFP-PCV1 ORF3 construct has a distinct cytoplasmic localization in transformed H1299 cells (Figure 2)[5]. As seen in Column 2 of Figure 2, the full-length PCV1 VP3 has localizes to the cytoplasm in H1299 cells.

To address this localization difference observed in transformed cells, primary foreskin fibroblasts (PFFs) were transfected with full-length PCV1 VP3. 24 hours after transfection, the PFF cells were fixed and GFP-PCV1 VP3 expression was observed by epifluorescence microscopy (Figure 2). As seen in the first column of Figure 2, the full-length PCV1 VP3 protein exhibits a distinct cytoplasmic localization in primary foreskin fibroblasts as well. In parallel to characterizing the subcellular localization of GFP-PCV1 VP3 in primary and transformed H1299 cells, PFFs were transfected with the p3XFLAG-*myc*-CMV-26-PCV1 ORF3 vector. This plasmid, previously constructed in the Heilman lab, had been used to measure the apoptotic induction ability of the full-length PCV1 VP3 protein in transformed H1299 cells[5, 16]. As described in Materials and Methods, the PFF cell line was transfected with a p3xFLAG control and a FLAG-PCV1 ORF3 construct, and assessed for cell death after 24 hours. As seen in Figure 3, the full-length PCV1 VP3 protein doesn't induce apoptosis in primary cells, as opposed to its high apoptotic induction in transformed H1299 cells.

Both figures discussed above indicate that PCV1 VP3 is similar to apoptin in terms of inducing apoptosis specifically in transformed cells. However, though both proteins have a cytoplasmic localization in primary cells, PCV1 VP3 differs in its localization in transformed cells compared to apoptin. The y-axis in Figure 3 measures the relative fluorescence due to the activation of effector caspases 3 and 7, which are involved in the downstream cascade of apoptosis pathways. The bar graph for H1299

13

cells transfected with PCV1 VP3 has a significantly higher RFU than transfected PFF cells, indicating that, like apoptin, PCV1 VP3 induces apoptosis specifically in transformed cells. Due to the observed localization differences, the data presented in Figures 2 and 3 thus suggests that the mechanism of apoptotic induction by PCV1 VP3 may be different from that of apoptin. Furthermore, the cytoplasmic localization observed in both primary and transformed H1299 cells suggests the presence of a functional nuclear export signal (NES) sequence in PCV1 VP3.

As shown in Figure 4, the ORF3 encoding the VP3 proteins in CAV, PCV1, and PCV2b shares homology in the N-terminal domain, especially in the NES sequence. However, PCV1 ORF3 encodes has a hydrophobic C-terminal tail domain, which encodes a protein twice the length of PCV2b VP3. Thus, to better understand the apoptosis-inducing mechanism of PCV1 VP3, to reveal if the NES sequence is functional, and to uncover the importance of the unique tail domain in localization and function, the NES and tail regions of PCV1 VP3 were identified and isolated to create truncation mutants. These mutants will ultimately be ligated into GFP vectors to facilitate localization detection once they are transfected into transformed H1299 cells.

To generate these PCV1 VP3 truncation mutants for localization studies, PCR was used to isolate and selectively amplify two regions of ORF3 coding for the putative NES sequence and the hydrophobic C-terminal tail domain of the protein. As described in the Materials and Methods section, primers were designed to amplify the ORF3 region coding for the first 63 amino acids, containing the nuclear export signal of VP3, and the last 102 amino acids, corresponding to the elongated tail domain of the protein. Products of the PCR reaction were characterized by electrophoretic separation on a 0.9% agarose gel. Since EcoRI and BamHI sequences were engineered into the PCR primers to facilitate truncation product ligation into T-vector, the expected sizes of the NES and tail mutants are approximately 210 and 325 nucleotides, respectively. As shown in Figure 5A, expected band sizes for PCV1 tail and NES truncation mutants, as well as the full-length PCV1 VP3 are visible in lanes 2-4, respectively, so the PCR amplification of the mutants was successful. The PCV1 tail band in lane 2 is between 0.3 and 0.4kb, the PCV1 NES mutant is between 0.2 and 0.3kb, and the full length PCV1 VP3 band is a slightly larger than 0.6kb.

14

To stabilize the purified truncation mutants and facilitate the amplification of our NES and tail regions of interest in bacterial cells, an intermediate vector was used to ligate the fragments into. The T-vector was chosen as it not only stabilizes the truncation mutants and makes it easy to amplify the gene of interest in bacteria, but its restriction efficiency is high as it creates sticky ends for subsequent ligation into GFP vector. Thus, to amplify the PCR products as part of a plasmid in bacterial cells, the purified NES and tail truncation mutants were inserted into an intermediate T-vector and transformed into the DH5α *E.coli* strain. Restriction digests with EcoRI and BamHI were performed on the T-vector constructs harvested from positive colonies to check for the presence of the NES and tail fragments. As seen on the agarose gel in Figure 5B, electrophoretic separation of the NES (lanes 3-5) and tail (lanes 7-9) restriction digests shows two bands of differing size in each lane. The top bands in lanes 3 to 5 and lanes 7 to 9, slightly above the marker band corresponding to 3 kb, appear to be of similar size. These bands represent the linearized T-vector with the PCR products restricted out. The bottom bands in lanes 3 to 5, slightly below the marker band corresponding to 0.3 kb, appear to be of the same size and represent the 210 nucleotide NES fragment. The bottom bands in lanes 7 to 9, slightly above the marker band corresponding to 0.3 kb, appear to be of the same size and represent the 325 nucleotide tail fragment. The bands seen on the gel confirm that truncation mutants of the appropriate length were successfully ligated into T vector, and subsequently restricted. Furthermore, sequencing of the purified restrictions of the fragments showed that no mutations were introduced during the isolation, amplification, and restriction process.

To allow for subcellular localization studies in transfected cells, the purified NES and tail fragments with the engineered EcoRI and BamHI cut sites needed to be ligated into a final vector which will facilitate detection of their localization. Since the GFP protein is very easy to track in cells the pEGFP-C1 vector was used to create fusion proteins with the NES and tail fragments. The vector creates an N-terminal GFP tag on the target protein. Thus, the truncation mutants were ligated into the EcoRI and BamHI restricted, linearized pEGFP-C1 vector. Successful ligation of the PCV1 truncation mutants into the GFP vector was tested by restriction enzyme digestion (Figure 5C). Lane 2 shows the expected band sizes for both the linearized GFP vector (~ 6kb) and the

15

restricted tail fragment slightly below the 0.4 kb marker band. Lane 3 was an unrestricted negative control so only one band should be visible. As expected, a band slightly above the 6 kb marker band is visible, corresponding to the circular GFP-PCV1 tail construct. Lane 4 shows the expected band sizes for both the linearized GFP vector (~ 6kb) and the restricted NES fragment slightly above the 0.2 kb marker band. Like Lane 3, Lane 5 was also a negative control. As expected, a band slightly above the 6 kb marker band is visible, corresponding to the circular GFP-PCV1 NES construct.

GFP fused to PCV1 truncation mutants will improve the study of the functionality and localization of the NES and the tail domain in transformed cells by facilitating their localization detection and tracking. Thus, with the successful creation of GFP-PCV1 truncation mutant constructs, transformed H1299 cells were transfected to visualize where the NES and tail fragments of PCV1 VP3 localize. 24 hours after transfection, the H1299 cells were fixed and GFP-PCV1 NES and GFP-PCV1 tail expression was observed by epifluorescence microscopy. Since GFP is small enough to freely diffuse in and out of the nucleus, the GFP control in transformed H1299 cells exhibits a diffuse localization pattern (column 1 of Figure 6). Observation of the GFP-PCV1 NES construct suggests a diffuse localization pattern, similar to the GFP control (column 2 of Figure 6). However, the NES seems to favor the nucleus as the intensity of the GFP signal is higher in the nucleus compared to the cytoplasm, suggesting that the NES sequence may not be functional. Meanwhile, as seen in column 3 of Figure 6, the GFP-PCV1 tail construct shows a distinct cytoplasmic localization, perhaps due to the numerous hydrophobic amino acid residues in the tail domain of the VP3 protein.

Since epifluorescence microscopy visualizes multiple focal planes and doesn't allow for Z-stack analysis, the observed localization may not be entirely accurate. In order to better characterize the subcellular localization of the PCV1 truncation mutants in transformed cells, confocal microscopy was used to visualize the GFP-PCV1 NES and GFP-PCV1 tail constructs (Figure 7). The third row of both columns, showing the merge of the blue, nuclear DAPI staining and the green GFP staining, gives the clearest indication of the localization of the NES and tail fragments. As seen in the bottom panel in Column 1, the GFP-PCV1 NES construct exhibits a diffuse localization pattern, but seems to favor the cytoplasm (Figure 7). This differs from the NES fragment localization

16

observed by epifluorescence microscopy (Figure 6), where the diffuse NES localization pattern seemed to favor the nucleus. Since the confocal microscope can take images of thin slices of the cell, the favored cytoplasmic localization of the NES fragment suggests that the hydrophobic tail may help with nuclear export. As was also seen in Figure 6, the bottom panel of Column 2 reiterates that the PCV1 tail fragment fused to GFP exhibits a distinct cytoplasmic localization (Figure 7). This cytoplasmic localization is reminiscent of the localization observed in Figure 2 with full-length PCV1 VP3 transfected into primary and transformed cells. The tail fragment is seen to be vesicular and highly cytoplasmic, suggesting that the tail domain may help to confer cytoplasmic localization to the full-length VP3 protein.

Discussion

Recent research has shown that PCV1 VP3 has a similar sequence homology to CAV VP3 and PCV2b VP3[16]. All three proteins seem to cause apoptosis in transformed cells, but their localization in primary and transformed cells differs. Apoptin localizes to the cytoplasm in primary cells, but its nuclear localization in transformed cells has been shown to be necessary for the induction of apoptosis[7]. Meanwhile, PCV1 VP3 and PCV2b VP3 have been shown to localize to the cytoplasm in both primary and transformed H1299 cells[2, 5]. Since all three proteins cause apoptosis in transformed cells, this differing localization implies that the inherent mechanisms of apoptotic induction may be dissimilar, or different than previously characterized. The mechanism by which PCV1 VP3 induces apoptosis is not yet known, so the purpose of creating truncation mutants was to gain insight into this mechanism as well as expand the comprehension of PCV2b VP3 and apoptin-mediated apoptosis.

We were able to observe the subcellular localization of the full-length PCV1 VP3 protein in primary cells. As shown in Figure 2, the full-length protein is completely cytoplasmic, similar to the localization observed in transformed H1299 cells[5]. This implies that the mechanism for apoptotic induction may be different from that of apoptin, which localizes to the nucleus in transformed cells. On the other hand, it is also possible

that the mechanism of apoptin may not be fully understood and correctly characterized, so its nuclear localization in transformed cells may be irrelevant.

Based on the images in Figure 6, the NES segment of the protein appears to be diffuse throughout the cell, similar to the GFP control. The confocal microscopy images also showed a diffuse localization pattern but the NES truncation mutant seems to be favoring the cytoplasm (Figure 7). From these observations, we hypothesize that the NES is functional. Though its localization appears to be diffuse when looked at under an epifluorescence microscope, Z-stack analysis on a confocal microscope shows that there is a greater concentration of the NES present in the cytoplasm than in the nucleus. Though the GFP protein is small enough to freely diffuse in and out of the nucleus, the fact that the GFP-PCV1 NES fusion protein seems to accumulate more in the cytoplasm leads us to believe that a functional NES is bringing the diffuse fusion protein out of the nucleus.

Interestingly, the tail portion of the PCV1 VP3 protein is entirely cytoplasmic (Figures 6 and 7). Since it has been truncated in the NES mutant, we believe that the tail domain may be necessary for full cytoplasmic localization. The C-terminal tail domain is highly hydrophobic, with many isoleucine, leucine, valine, and phenylalanine amino acid residues. The confocal images in Figure 7 depict the cytoplasmic localization nature of the tail portion. The hydrophobic tail forms vesicular structures and is totally absent from the nucleus. As previously discussed, the full-length protein is also completely absent from the nucleus in both primary and transformed cells (Figure 2). However, it is interesting to note that in primary cells the VP3 protein has a punctate distribution all around the nucleus. Meanwhile, both the full-length protein and the tail truncation mutant in transformed cells seem to be vesicular and form foci. The differing cytoplasmic distribution in primary versus transformed cells may be due to inherent differences between these cell types. Based on these observations, we believe it is likely that the vesicular structure seen in the tail truncation mutant may help confer cytoplasmic localization of the full-length PCV1 VP3 protein. Another possibility is that the NLS of the VP3 may not be functional, or that the tail blocks NLS activity and import of the protein into the nucleus.

A noteworthy future experiment would be an analysis of the localization of the putative NLS, as well as the 5' region of PCV1 VP3 with the entire tail domain removed. Epifluorescence and confocal imaging could be performed on both primary and transformed cells transfected with these mutants to give insight on the localization of the functional sequences, as well as an indication of the importance of the tail region. If the NLS is functional, we would expect the NLS mutant to localize to the nucleus in both primary and transformed cells. However, for the truncation mutant with the entire tail domain removed, we would expect it to favor cytoplasmic localization in both cell types because the NES truncation mutant and full-length protein exhibit a cytoplasmic accumulation. A minor experiment could be done with our NES and tail truncation mutants transfected into primary cells, to assess whether localization of these mutants differs in any way between primary and transformed cells.

To glean more insight into the various regions of the VP3 protein and their localization and function, DsRed could be used along with GFP for parallel localization studies. For instance, the tail truncation mutant could be cloned into the DsRed vector while the mutant with the tail domain removed could be cloned into the GFP vector. The two vectors could be transfected into the same cells to compare localization in the same microenvironment. It would be interesting to see whether the mutants multimerize and recover the localization and functionality of the full-length protein. Additionally, other cellular organelles could be stained for during localization studies. Since the tail truncation mutant seems to be vesicular, a future experiment could stain for the Golgi apparatus to see whether the tail domain goes into these complexes for processing and packaging into vesicles.

In addition to the localization studies, an apoptosis assay was performed with full-length PCV1 VP3 in primary cells (Figure 3). Grouped with data collected last year in the Heilman lab, we were able to demonstrate that PCV1 VP3 apoptosis is specific to transformed cells[16]. The transformed cells used were H1299, a non-small cell lung carcinoma cell line that is p-53 null. H1299 cells provide a reasonable foundation for the study as they exhibit many characteristics typical of transformed cells, including adherence and immortality. These cells have been used to research apoptin, which has been shown to induce apoptosis in H1299 and many other transformed cell types. As seen

in Figure 3, the level of fluorescence in the transformed cells was significantly higher than the primary cell line used, PFF. Thus PCV1 VP3 follows the trend of PCV2b VP3 and CAV VP3 apoptotic induction in transformed cells. However, the differing localization of the three VP3 proteins leads us to believe that compared to apoptin, PCV1 VP3 and PCV2b VP3 employ alternative mechanisms of apoptotic induction. To uncover more information on PCV1 VP3's apoptosis-inducing mechanism, future experiments could look to use our NES and tail truncation mutants to perform apoptosis assays in both PFF and H1299 cell lines. Since the tail truncation mutant had a distinctly cytoplasmic localization, and seemed to form foci and be vesicular, we hypothesize that it may be involved in the activation or enhancement of PCV1 VP3-induced apoptosis. The apoptosis assay with truncation mutants would provide information on whether the apoptotic characteristics seen in the full-length VP3 protein remain present, and if the tail domain may have a positive, enhancing effect on apoptotic induction[4].

It is also interesting that the VP3 protein of all three viruses seems to be able to induce apoptosis in a p-53 independent manner since it kills H1299, p-53 null cells. Furthermore, the use of a caspase-3/7 apoptosis assay to measure fluorescence suggests that these effector caspases are involved in the downstream apoptotic cascade mechanism in PCV1 VP3. Previously, caspase-3 has been shown to be involved in the apoptotic induction mechanism of apoptin, and PCV2b VP3 apoptotic activity has also been measured with a caspase-3/7 apoptosis assay[2, 8]. Since caspase-3 seems to be involved in the apoptotic cascade of the three VP3 proteins, further studies should look into the importance of caspases 3 and 7 in the apoptotic induction mechanisms of all three viral proteins.

Based on our results we are able to conclude that the full length PCV1 VP3 protein localizes to the cytoplasm of primary and transformed cells, and seems to induce apoptosis specifically in transformed cells. The localization studies on truncation mutants proved the NES is diffuse in transformed cells, but favors the cytoplasm. The tail region may assist in cytoplasmic localization of the full-length protein, as it localizes in vesicular structure lies outside of the nucleus. These results also set up the possibility for various future experiments and add information to the field regarding the similarities and differences of the VP3 proteins of CAV, PCV1, and PCV2b. As more research is

conducted, a better idea of the mechanism of PCV1 VP3 apoptotic induction will be revealed, and the protein may prove beneficial in the world of oncological medicine.

Figures
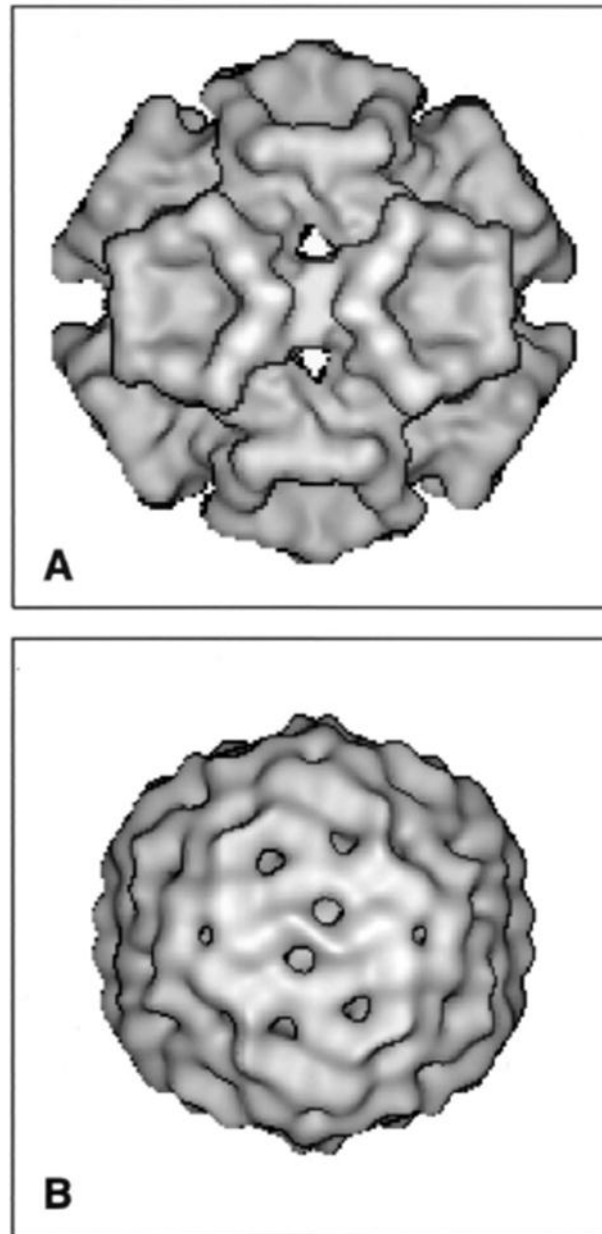
Figure 1: Images of circoviruses showing three-dimensional maps.

A) CAV image computed from cryomicrographs. B) PCV2 image computed from cryomicrograps[6].
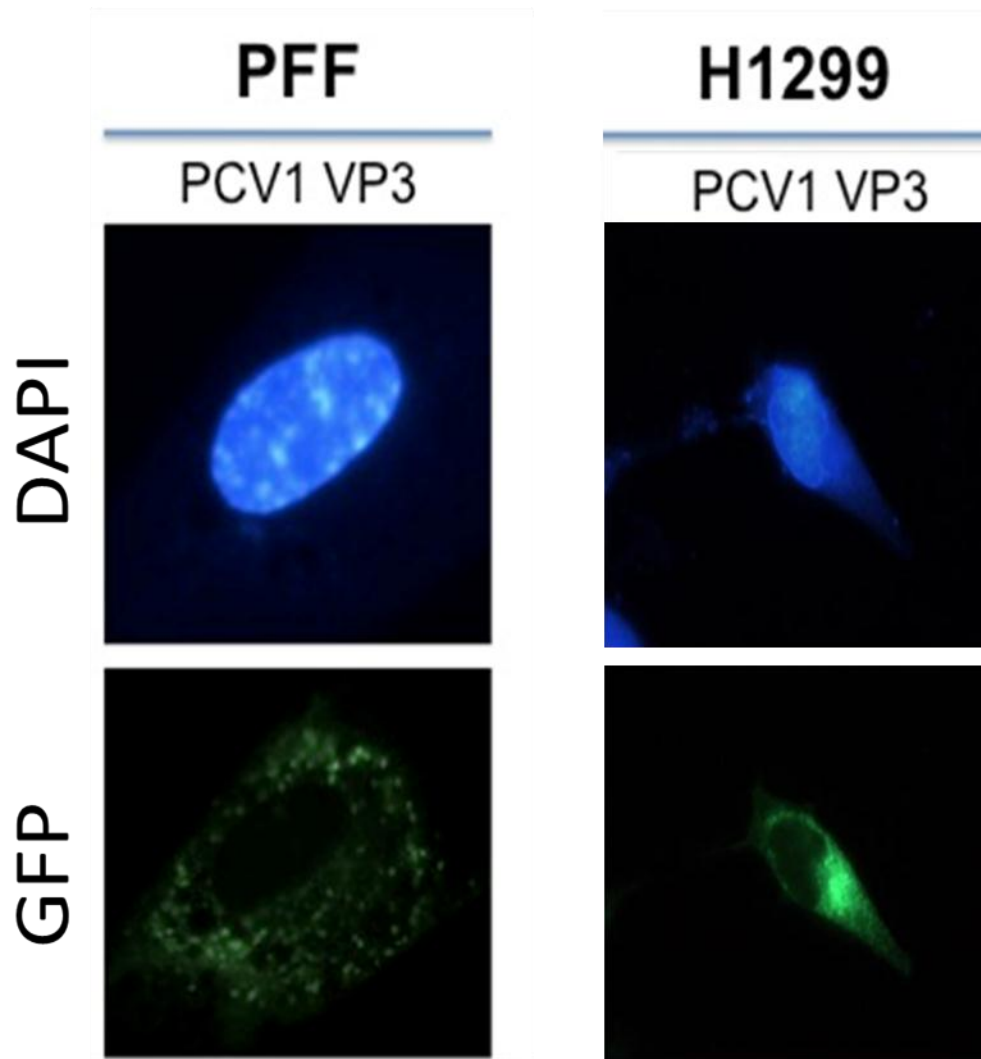
Figure 2: Epifluorescense imaging of cell nuclei (DAPI, blue) and GFP (green).

Full-length PCV1 VP3 in primary foreskin fibroblasts (PFF) has a distinct cytoplasmic localization. The protein has a similar localization in transformed H1299 cells, accumulating in the cytoplasm.
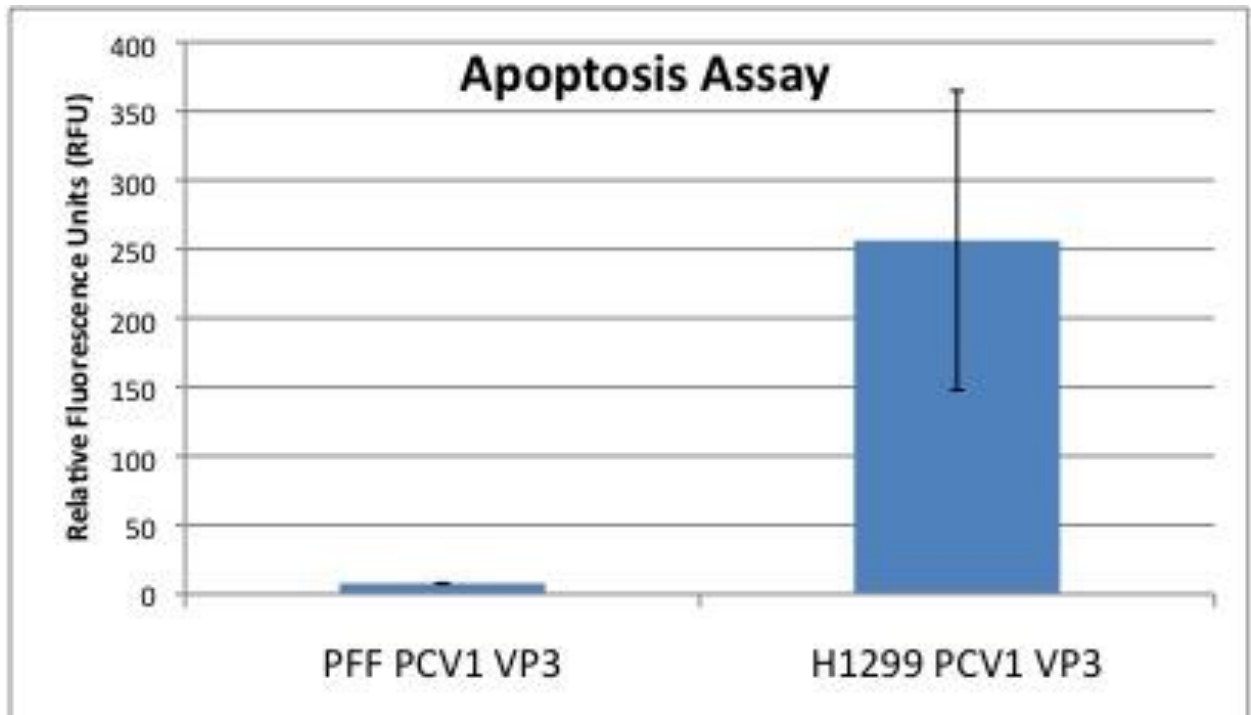
Figure 3: Apoptosis assay for FLAG control and full-length PCV1 VP3 in primary foreskin fibroblasts (PFF) and H1299 cells.

After transfection the cells were incubated for 24 hours before the apoptosis assay was performed. Fluorescence is due to caspase 3/7 activation. Apoptosis observed with FLAG background controls was subtracted out to normalize the data. Relative fluorescence units were measured, showing that PCV1 VP3 doesn't induce apoptosis in primary cells, as opposed to its high apoptotic induction in transformed H1299 cells.
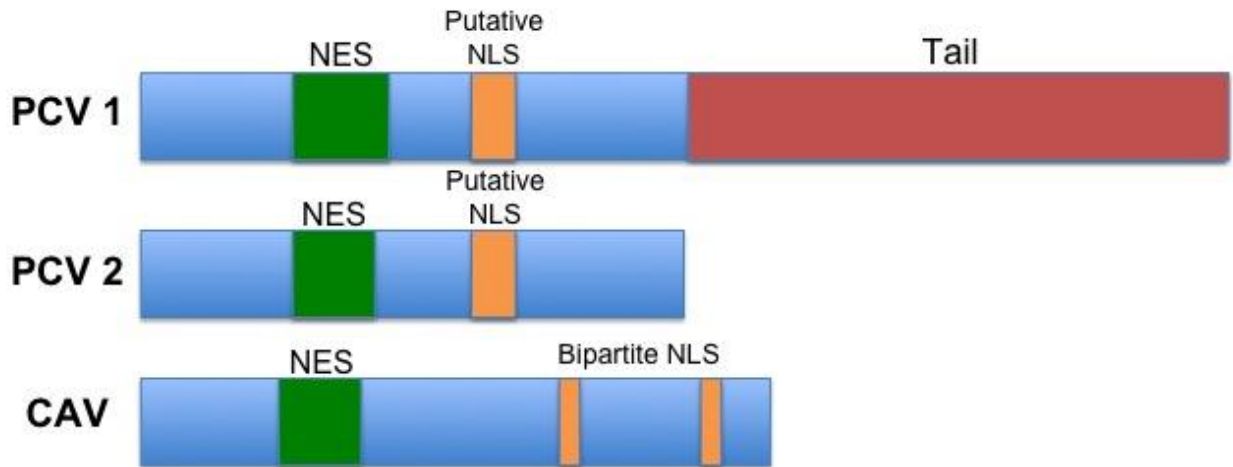
Figure 4: Comparison of the lengths of PCV1, PCV2 and CAV ORF3.

The schematic shows the NES sequence homology in the N-terminus, putative NLS location and the C-terminal tail domain of PCV1 ORF3.
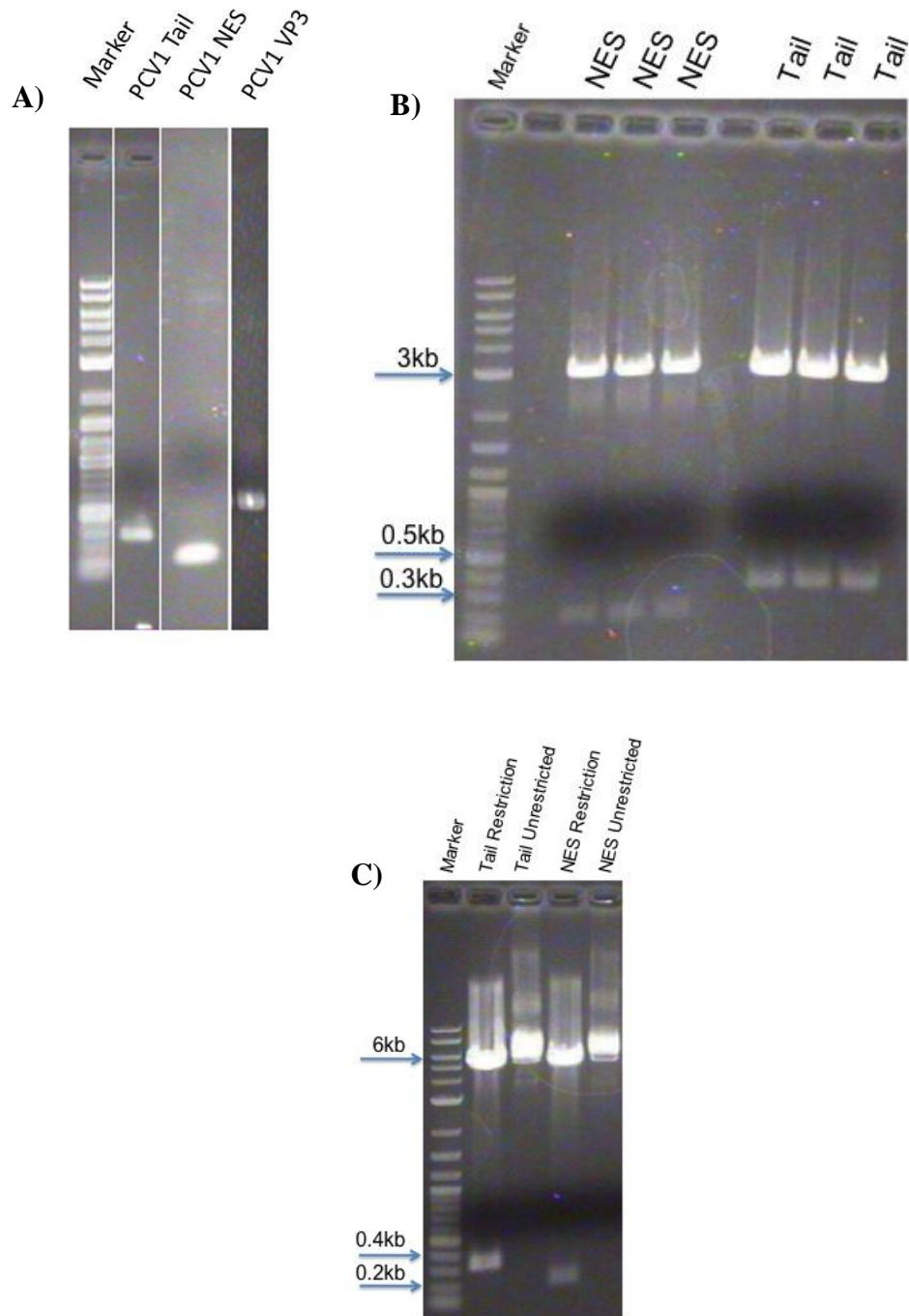
Figure 5: Agarose Gel Electrophoresis.

A) PCR products were purified using agarose gel electrophoresis. Lanes 2-4 show expected band sizes for tail (~0.3kb) and NES (~0.2kb) PCR fragments, as well as full-length PCV1 VP3 (~0.6kb). B) Agarose gel electrophoresis on T-vector restriction products showing expected band sizes of NES and Tail truncation mutants. C) pEGFP vector restrictions showing NES and Tail mutants successfully ligated into the GFP plasmid.
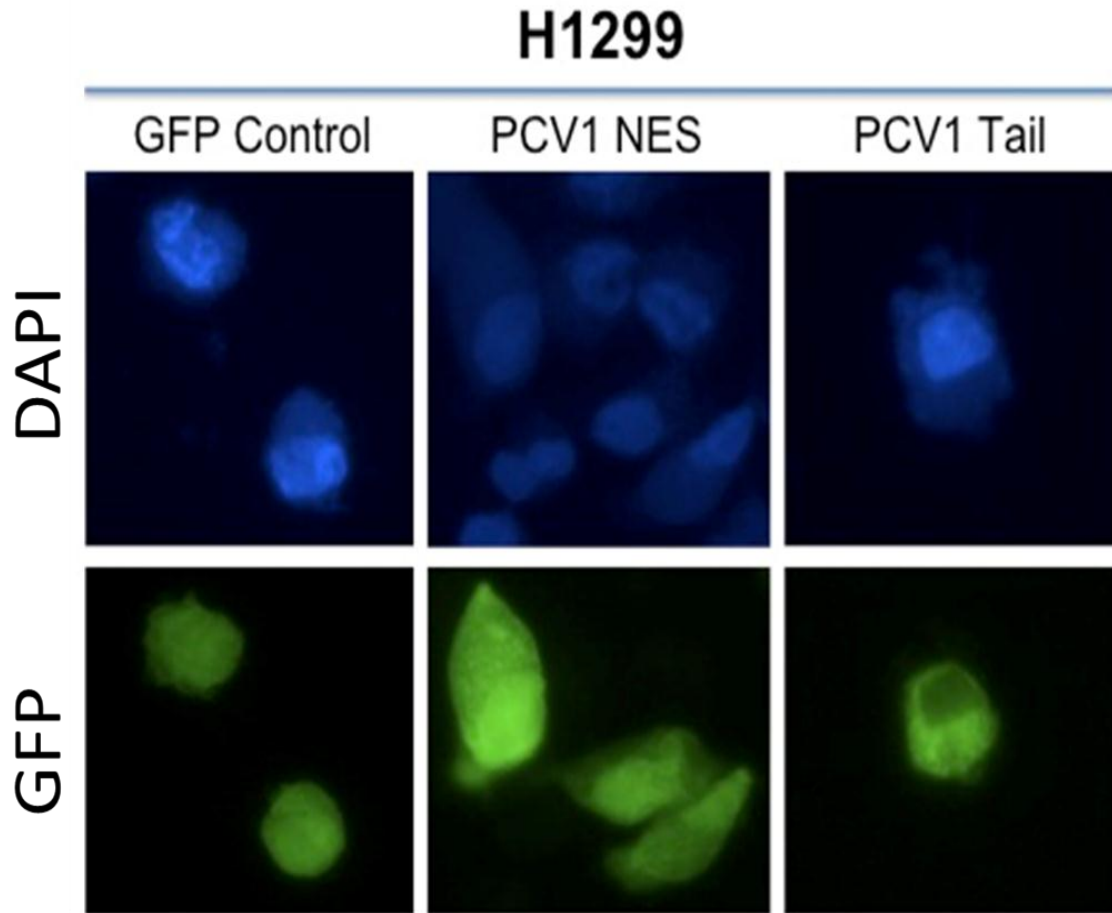
Figure 6: Epifluorescence imaging of H1299 cell nuclei (DAPI, blue) and GFP (green).

Full-length PCV1 VP3 in primary foreskin fibroblasts has a distinct cytoplasmic localization. The GFP control is diffuse throughout the transformed H1299 non-small cell lung carcinoma cells. The NES truncation mutant seems to be diffuse throughout the cell, similar to the GFP control. The tail mutant has a distinct cytoplasmic localization.
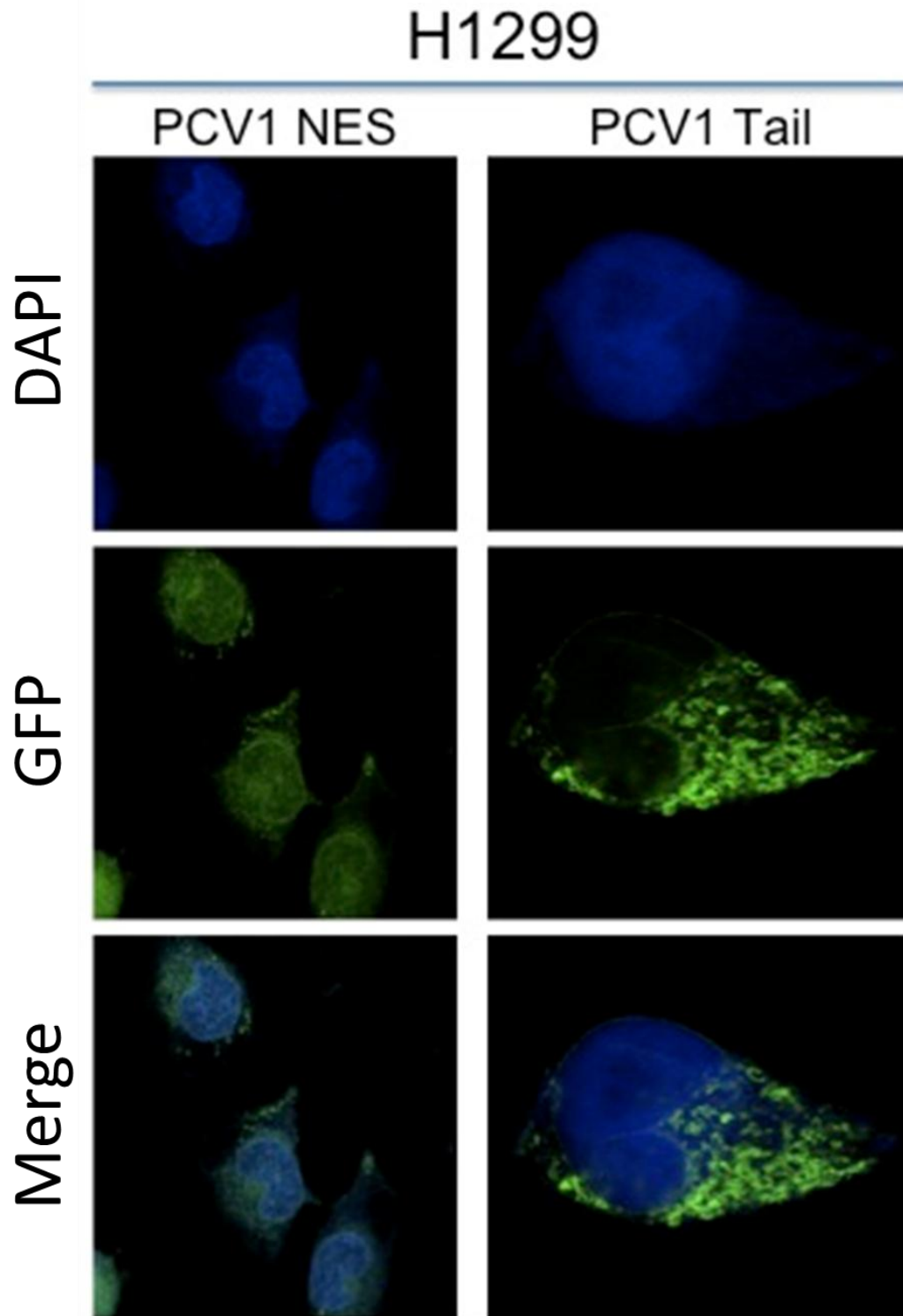
Figure 7: Confocal fluorescence imaging of cell nuclei (DAPI, blue) and GFP (green).

The tail domain is shown to be vesicular and strictly cytoplasmic. The NES is found mainly in the cytoplasm, though some green staining is visible in the nucleus.

References

1. **Baker, D.J., Dawlaty, M.M., Galardy, P., van Deursen, J.M.** 2007. Mitotic regulation of the anaphase-promoting complex. Cell. Mol. Life Sci. **64**: 589-600.

2. **Bourque, J., Goldstein, J., Heilman, D.H.** 2008. Cloning and structure-function analysis of porcine circovirus 2 VP3. Major Qualifying Project, Worcester Polytechnic Institute, Worcester, MA.

3. **Brasefield, J., Tischer, D., Heilman, D.H.** 2009. Exploring Apoptin's Anticancer Ability: Uncoupling Nuclear Export and Multimerization. Major Qualifying Project, Worcester Polytechnic Institute, Worcester, MA.

4. **Chaiyakul, M., Hsu, K., Dardari, R., Marshall, F., Czub, M.** 2010. Cytotoxicity of ORF3-proteins from a non-pathogenic and a pathogenic Porcine circovirus. J. Virol. **10:** 1128.

5. **Conerly, P., McShea, M.** 2009. Cloning and Expression of PCV1 ORF3. Major Qualifying Project, Worcester Polytechnic Institute, Worcester, MA.

6. **Crowther, R.A., Berriman, J.A., Curran, W.L., Allan, G.M., Todd, D.** 2003. Comparison of the Structures of Three Circoviruses: Chicken Anemia Virus, Porcine Circovirus Type 2, and Beak and Feather Disease Virus. Journal of Virology. **77-24:** 13036-13041.

7. **Danen-Van Oorschot, A. A., Fischer, D.F., Grimbergen, J.M., Klein, B., Zhuang, S., Falkenburg, J.H., Backendorf, C., Quax, P.H., Van der Eb, A.J., Noteborn, M.H**. 1997. Apoptin induces apoptosis in human transformed and malingant cells but not in normal cells. Proc. Natl. Acad. Sci. USA. **94**: 5843-5847.

8. **Danen-van Oorschot, A.A.A.M., van der Eb, A.J., Noteborn, M.H.M.** 2000. The Chicken Anemia Virus-Derived Protein Apoptin Requires Activation of Caspases for Induction of Apoptosis in Human Tumor Cells. Journal of Virology. **74-15:** 7072-7078.

9. **Faurez, F., Dory, D., Grasland, B., Jestin, A.** 2009. Replication of Porcine Circoviruses. Virology Journal **6:** 60.

10. **Fenaux, M., Opriessnig, T., Halbur, P.G., Meng, X.J.** 2003. Immunogenicity and Pathogenicity of Chimeric Infectious DNA Clones of Pathogenic Porcine Circovirus Type 2 (PCV2) and Nonpathogenic PCV1 in Weaning Pigs. Virology **77-7:** 11232–11243.

11. **Heilman, D., Teodoro, J.G., Parker, A.E., Green, M.R.** 2004. The viral Protein Apoptin Associates with the Anaphase-promoting Complex to Induce G2/M Arrest and Apoptosis in the Absence of p53. Genes Dev. **18**: 1952-1957.

12. **Heilman, D. W., Teodoro, J., Green, M.** 2006. Apoptin Nucleocytoplasmic Shuttling Is Required for Cell Type-Specific Localization, Apoptosis, and Recruitment of the Anaphase-Promoting Complex/Cyclosome to PML Bodies. Journal of Virlogy **80-15**: 7535–7545.

13. **Hutten, S., Kehlenback, R.H.** 2007. CRM1-mediated nuclear export: to the pore and beyond. Trends in Cell Biology. **17-4:** 193-201.

14. **Israels, L.G., Israels, E.D.** 1999. Apoptosis. The Oncologist **4**: 332-339.

15. **Kiupel, M., Stevenson, G.W., Galbreath, E.J., North, A., HogenEsch, H., Mittal, S.** 2005. Porcine Circovirus type 2 (PCV2) causes apoptosis in experimentally inoculated BALB/c mice. BMC Veterinary Research. **1:**7.

16. **Kokolis, J., Spada, L., Heilman, D.H.** 2010. Assessing the Functionality of Localization Sequences Isolated from PCV1 VP3. Major Qualifying Project, Worcester Polytechnic Institute, Worcester, MA.

17. **Liu, J., Chen, I., Kwang, J.** 2005. Characterization of a Previously Unidentified Viral Protein in Porcine Circovirus Type 2-Infected Cells and Its Role in Virus-Induced Apoptosis. Journal of Virology **79-13**: 8262–8274.

18. **Liu, J., Chen, I., Du, Q., Chen, H., Kwang, J.**. 2006. The ORF3 Protein of Porcine Circovirus Type 2 Is Involved in Viral Pathogenesis In Vivo. J. Virol. **80**: 5065-5073.

19. **Liu, J., Zhu, Y., Chen, I., Lau, J., He, F., Lau, A., Wang, Z., Karuppannan, A.K., Kwang, J.** 2007. The ORF3 Protein of Porcine Circovirus Type 2 Interacts with Porcine Ubiquitin E3 Ligase Pirh2 and Facilitates p53 Expression in Viral Infection. J. Virol. **81**: 9560-9567.

20. **Los, M., Panigrahi, S., Rashedi, I., Mandal, S., Stetefeld, J., Essmann, F., Schulze-Osthoff, K.**. 2009. Apoptin, a tumor selective killer. Molecular Cell Research. **1798-8**: 1335-1342.

21. **Noteborn, M.H.M., Todd, D., Verschueren, C.A.J., de Gauw, H.W.F.M. Curran W.I., Veldkamp, S., Douglas A.J., McNulty, M.S., Van der Eb, A.J., Koch, G.** 1994. A single chicken anemia virus protein induces apoptosis. J. Virol. **68:** 346-351.

22. **Phenix, K. V., Weston, J. H., Ypelaar, I., Lavazza, A., Smyth, J. A., Todd, D., Wilcox, G.E., Raidal, S.R.** 2001. Nucleotide sequence analysis of a novel circovirus of canaries and its relationship to other members of the genus Circovirus of the family Circoviridae. Journal of General Virology. **82:** 2805-2809.

23. **Rosenberger, J.K., Cloud, S.S.** 1998. Chicken Anemia Virus. Poultry Science. **77:** 1190-1192.

24. **Sherr, C. J.** 2004. Principles of tumor suppression. Cell. **116**: 235–246.

25. **Steinfeldt, T. Finsterbusch, T. Mankertz, A**. 2001. Rep and Rep' Protein of Porcine Circovirus Type 1 Bind to the Origin of Replication in Vitro. Virology **291**: 152-160.

26. **Steinfeldt, T., Finsterbusch, T., Mankertz, A.** 2007. Functional Analysis of cis- and trans-Acting Replication Factors of Porcine Circovirus Type 1. Journal of Virology. **81:** 5696-5704.